doi:10.1017/S1431927614011350
Microsc. Microanal. 20 (Suppl 3), 2014

Multilayered Cr(Al)N/SiO$_x$ Nanocomposite Coatings Fabricated by Differential Pumping Cosputtering.

Masahiro Kawasaki[1], Masateru Nose[2], Ichiro Onishi[3] and Makoto Shiojiri[4]*

[1]. JEOL USA Inc., 11 Dearborn Road, Peabody, MA 01960, USA.
[2]. Faculty of Art and Design, University of Toyama, Takaoka, Toyama 933-8588, Japan.
[3]. JEOL Ltd. 3-1-2 Musashino, Akishima, Tokyo 196-8558, Japan
[4]. Kyoto Institute of Technology, Kyoto 606-8585, Japan.
* Present address: 1-297 Wakiyama, Kyoto 618-0091, Japan.

Nanocomposite films of metal nitrides such as TiN/Si_3N_4, TiN/BN, and CrN/AlN have attracted substantial attention as coating materials for improving hardness and saving rare metals. It is difficult to prepare composite films consisting of nitride and oxide by conventional reactive sputtering methods. Nose *et al.* developed a differential pumping cosputtering (DPCS) system, which can fabricate different nanocomposite films [1]. To elucidate the process and mechanism of film growth in the DPCS system, we prepared a hard coating Cr(Al)N/SiO$_x$ nanocomposite layer on the under buffer layers that were grown on a Si substrate and have been examining by means of analytical electron microscopy.

The DPCS system has two chambers **A** and **B** for radio frequency (RF) sputtering of different materials and a substrate holder rotating, as shown in Figure 1 [1]. $Cr_{50}Al_{50}$ and SiO_2 targets were set in chambers **A** and **B,** respectively, and (001) Si wafers were used as the substrates. The substrates were heated at 250°C and rotated at a speed of 1 rpm. First, three depositions were successively performed on the Si substrate by sputtering only from the CrAl target in chamber **A,** with different gas flows. They are the transition layers to promote adhesion between the composite layer and substrate [2, 3]. Next, the main deposition was carried out for 660 min by operating both the CrAl chamber **A** and the SiO_2 chamber **B,** on the transition layers rotated at the same speed. The CrAl sputtering and the SiO_2 sputtering were performed with flows of Ar (10 sccm)+N2 (20 sccm) and Ar (20 sccm) at RF powers of 200 and 75 W, respectively, so as to obtain a nominal composition of Cr(Al)N/38 vol.% SiO$_x$. Analytical electron microscopy was performed with a JEM-2800, attached with a JEOL 100 mm^2 Silicon Drift Detector (SDD) for energy dispersive X-ray spectroscopy (EDS), a Gatan GIF Tridiem for electron energy los spectroscopy (EELS), and an Orius 200D (model 833) for electron diffraction (ED), followed by atomic scale high-resolution (HR) investigation in a JEOL ARM200F equipped with a cold field emission gun.

An image of the coating (F) with the transition layers (B, C, D, and E) deposited on the Si wafer (A) is shown in Figure 2. Figure 3 shows a high-angle annular dark field (HAADF) scanning transmission electron microscopy (STEM) and the corresponding EDS of Si-K, O-K, Al-K, Cr-K and N-K signals, which indicate that dark bands ~1 nm thick in the HAADF image are rich with Si and O, while brighter dark bands ~1.6 thick are rich with Cr, Al, and N. EELS mapping in Figure 4 confirmed that Cr(Al)N layers included Cr and N atoms, since EDS maps sometimes display artifact [4]. The deposited layer looked to be a multilayered structure comprising Cr(Al)N layers and silicon oxide (SiO$_x$) layers. The Cr(Al)N was NaCl-typed CrN crystal containing some amounts of Al atoms, having a lattice parameter as small as 3 % compared with the pure CrN crystal, and the SiO$_x$ was amorphous (a), growing as separated island particles rather than continuous cover layer on the surface of the Cr(Al)N crystal layer in the columnar grains [2]. During the following CrAl deposition in chamber **A,** Cr(Al)N crystals could grow directly on surface areas of the under Cr(Al)N crystal where no a-SiO_x particles were deposited, keeping the coherent lattice relation, as seen in Figure 5.

The indentation hardness of the present sample, measured using a nanoindentation system (Fischerscope, H100C-XY_p), was as low as ~25 GPa. This is ascribed to the composition and the substrate rotation speed [3]. The hardness of Cr(Al)N/SiO_x coatings decreased monotonously from ~27 GPa for no fraction of SiO_x [Cr(Al)N] to ~10 GPa for pure SiO_x with increasing SiO_x fraction. The size and number density of *a*-SiO_x particles would increase with oxide fraction and then the continuous SiO_x layer might completely separate the CrAlN layers, decreasing the harness of the sample. The hardness of Cr(Al)N/38 vol. % SiO_x prepared at 12 rpm was ~33 GPa. Faster rotation would make a-SiO_x particles smaller, resulting in the formation of Cr(Al)N crystal including very fine *a*-SiO_x particles with small number density. Although a Cr(Al)N layer at each deposition was thin, the Cr(Al)N could grow as columnar crystalline grains because the opportunity for Cr(Al)N directly deposited on the surface of the under Cr(Al) layer was high due to the formation of only a few small a-SiO_x particles. These fine SiO_x particles can work as obstacles for the lattice deformation of the Cr(Al)N crystals so that they make the composite films harder. Indeed the hardness of a Cr(Al)N/17 vol. %SiO_x coating prepared at 12 rpm reached ~46 GPa. The hardness of this superhard nanocomposite coating was higher than that of Cr(Al)N coating ~43 GPa, which indicates the effect of *a*-SiO_x nanoparticles as the obstacles against lattice distortion. Hence the DPCS system has strong potentials to fabricate functional composite layers with physically, chemically and economically good properties such as hard or superhard nitride/oxide coatings.

[1] M. Nose *et al*, J. Vac. Sci. Technol. **A 30** (2012) 011502.
[2] M. Kawasaki *et al*, ACS Appl. Mater. Interfaces **5** (2013) 3833.
[3] M. Kawasaki *et al*, Appl. Phys. Lett. **103** (2013) 201913.
[4] M. Kawasaki *et al*, Appl. Phys. Lett. **102** (2013) 091603.

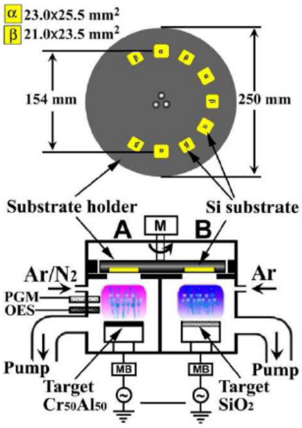

Fig. 1. DPCS system.

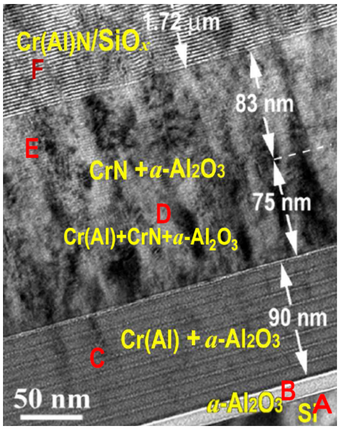

Fig. 2. Deposited layers.

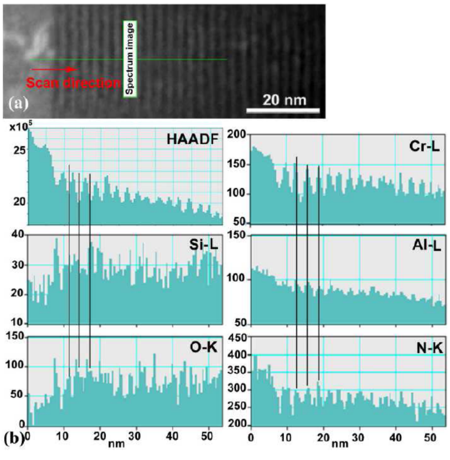

Fig. 3. HAADF image & EDS of the Cr(Al)N/SiO_x coating.

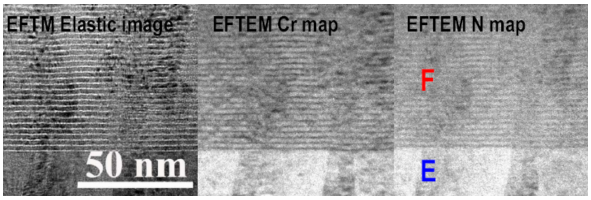

Fig. 4. EFTEM image and EELS maps of the coating.

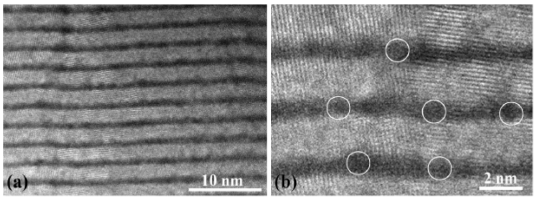

Fig. 5. HAADF images of the coating layer F.